ELSEVIER

Microelectronics Journal 30 (1999) 841–849

Microelectronics Journal

www.elsevier.com/locate/mejo

New precise SPICE macromodels for the current-feedback operational amplifier

M.H. Eltawil, A.M. Soliman*

Department of Electronics and Communications Engineering, Cairo University, Giza, Egypt

Accepted 11 January 1998

Abstract

Two new linear, frequency-dependent macromodels for the Current-Feedback Operational Amplifier (CFOA) are introduced. Both macromodels simulate the actual performance of typical CFOAs for a wide range of frequencies. The first proposed macromodel suits manual calculations due to its relatively simple mathematical model. The second proposed macromodel shows more accurate results but is described through a more complex set of mathematical equations. Both macromodels present performance advantages over previously introduced macromodels.

Keywords: Current feedback operational amplifier; SPICE macromodel

1. Introduction

The CFOA has emerged as one of the most important building blocks in the analog design library. Recently, the use of the CFOA as a four-terminal active building block has been highlighted [1] and used efficiently in developing many application based on the CFOA as the active building block. Testing the developed circuits is done usually using SPICE (Simulation Program with Integrated Circuit Emphasis) with a company specific model for the CFOA.

With the increasing complexity and shorter design cycles of today's designs, computer modeling with SPICE is becoming more popular. This is especially true with high-speed designs utilizing the latest in CFOAs. The need thus for accurate macromodels to model the actual performance of CFOAs have evolved as one of the growing needs both to obtain a trusted simulation of the required circuit and also to understand the limitations imposed on the operation due to the presence of parasitic effects. A simple macromodel that counts only for the currents and the voltage tracking errors was used [2–4] to model the actual performance of the CFOA. This model imposes no frequency limitations and its performance is far from the actual performance. Another model that counts for the basic parasitics was developed [5–7]. The model follows the actual performance for a limited range of frequencies. At low and high frequencies, the performance of the macromodel largely deviates from the actual performance. A third model that closely describes typical CFOAs was presented [8]. The model in [8] is fairly accurate for a good range of frequencies although it deviates from the actual performance at low frequencies. In this paper two new SPICE generic macromodels for the CFOA are presented. Both models use a lower number of elements than in [8] thus offers a shorter simulation time. The first proposed macromodel also is suitable for manual calculations due to the fairly simple mathematical equations used in describing the macromodel.

SPICE models are widely used to simulate circuit performance [8–13], but there is always the question of how well does the SPICE simulation results resemble the real responses. The most accurate model that can be trusted to a great extent is the transistor level model, a mapping of the amplifier internal structure actually manufactured using the parameters of the used technology of fabrication. A device-level model can accurately model all the practical aspects usually found in real life such as the variation of the performance with temperature, even the effects of devices mismatch and fabrication tolerances can be predicted using the Monte Carlo (MC) and the Worst Case (WC) analysis offered by SPICE.

It seems thus that the answer to the previous question is to use a device-level model.

2. The philosophy of macromodeling

Usually the philosophy involved in creating a

* Corresponding author.

0026-2692/99/$ - see front matter
PII: S0026-2692(99)00020-8

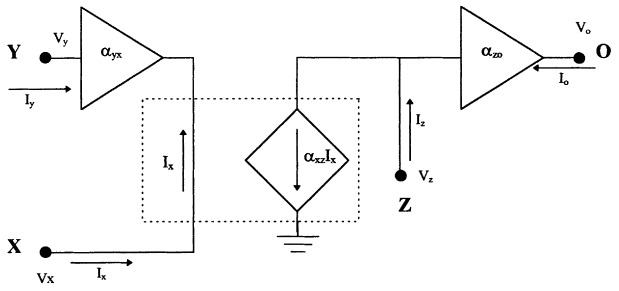

Fig. 1. A simple modeling of the non-idealities of the CFOA.

macromodel is the desire to design a model that would simulate the typical behavior of a CFOA while executing much faster than a device level model. Also, the macromodel would act as a development platform for effects not normally included in other simpler models such as temperature effects, noise, and many of the other second- and third-order effects that are typical to most common CFOAs. Such macromodels are usually supplied by the manufacturers and they are much compact than a device-level model, thus gain in simulation time can be achieved without sacrificing results fidelity.

In many cases, a detailed study of all practical aspects is not necessary, such as when designing a filter that will operate at a fixed well-defined temperature. The most important aspect in such a case is to study the non-ideal effects on the frequency performance of the given filter. The macromodels supplied by the manufacturers thus will be too complex as they model all the practical aspects of CFOAs.

The goal of this paper therefore is to develop a simple frequency dependent model that accurately models the frequency performance of most common CFOAs.

Several authors have introduced in the literature a simple modeling method based on counting for the currents and voltages tracking errors [2–4] (Fig. 1). The model contains three parameters to be determined by measurements i.e.

1. α_{yx}, the Y to X voltage gain,
2. α_{xz}, the X to Z current gain and
3. α_{zo}, the Z to O voltage gain.

All of the previously listed parameters are ideally unity.

The mathematical equations that describe the model can be given as

$$I_y = 0 \tag{1a}$$

$$V_x = \alpha_{yx} V_y \tag{1b}$$

$$I_z = \alpha_{xz} I_x \tag{1c}$$

$$V_z = \alpha_{zo} V_o. \tag{1d}$$

Measuring of the parameters is fairly easy, α_{yx} is measured by applying a voltage signal at port Y and measuring the resulted voltage at port X. α_{xz} is measured by injecting a current signal at port X and measuring the output current at port Z. Whereas α_{zo} is measured the same way as α_{yx}.

The aforementioned parameters measured for the AD844 from Analog Devices are given by

$$\alpha_{yx} = \alpha_{xz} = \alpha_{zo} \approx 1.$$

(Actually simulation shows that the aforementioned parameters deviate from unity by less than 0.1%.)

To test the accuracy of the model, simulation of the non-inverting differentiator shown in Fig. 2 was carried out for both the earlier model and the model given by Analog Devices in the PSpice library. The results are shown in Fig. 3. By examining the results one can conclude that the model is not accurate (the range of validity of the model is very small for the given circuit). One of the obvious drawbacks is that the model imposes no upper limitation on the maximum frequency of operation, which is expected for actual devices.

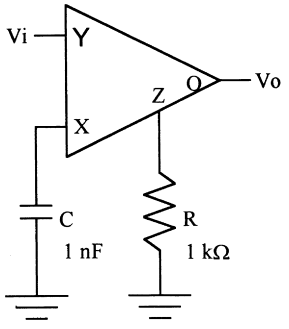

Fig. 2. The non-inverting differentiator used in testing the different macromodels.

3. Simple parasitic modeling

A better, yet very simple macromodel was proposed [5–7]. The model used is shown in Fig. 4. Clearly, it overcomes the leaks found in the previous model by introducing the following:

1. A finite, frequency dependent, open loop gain.
2. A dominant pole.
3. Finite input resistances for the voltage follower stages.

The mathematical equations that describe the model can be given as

$$I_y = 0 \tag{2a}$$

$$V_x = \alpha_{yx} V_y + R_x I_x \tag{2b}$$

$$I_z = \alpha_{xz} I_x + \left(\frac{1}{R_z} + sC_z \right) V_z \tag{2c}$$

$$V_o = \alpha_{zo} V_z + R_o I_o. \tag{2d}$$

The parameters of the model can be easily measured as follows:

1. R_x is measured with port Z open, port O open, port Y

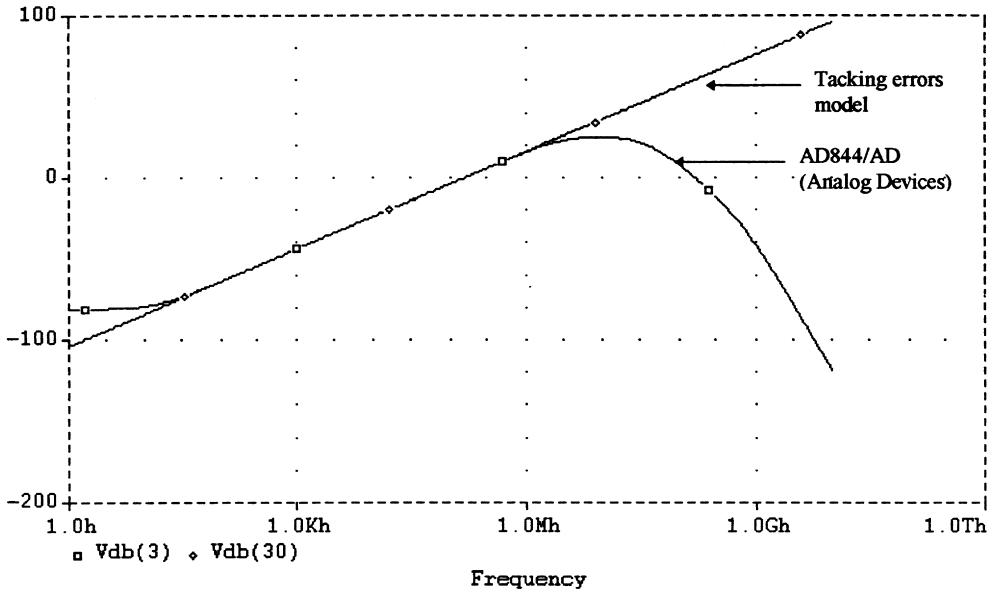

Fig. 3. The simulated response of the non-inverting differentiator shown in Fig. 2 for both the tracking errors model and the AD844/AD.

connected to a varying voltage source while port X is connected to ground. By measuring the current flowing from port X into ground, R_x can be determined.

2. The grounded impedance seen at port Z can be measured with port Y grounded, port O open and port X is connected to a varying current source. Dividing the voltage developed at port Z by the current flowing into port X, the impedance seen at port Z can be calculated.
3. The output resistance R_o can be measured in the same way as for R_x with ports X and Y grounded.

Measuring the aforementioned parameters for the AD844 from Analog Devices gives

$$R_x \approx 50\ \Omega, R_z \approx 3\ \mathrm{M}\Omega, C_z \approx 5\ \mathrm{pF} \text{ and } R_o \approx 15\ \Omega,$$

whereas the voltages and the current tracking constants are as before, almost unity.

To test the accuracy of the model, simulation of the same non-inverting differentiator shown in Fig. 2 was carried out for both the earlier model and the model given by Analog devices in the PSpice library. The results are shown in Fig. 5. By examining the results and comparing it to the previous model where only the tracking errors were modeled it is clear that that model behaves much closer to the AD844/AD model than the first one.

Although the model presented can be very useful when manual-solving problems like frequency limitations and stability analysis [13], yet it cannot give an accurate answer to the previous problems. To make the model simple for manual calculations several effects have been omitted, like the increase in the voltage follower output impedance with frequency and the finite voltage and current conveying properties.

4. Fabre and Alami macromodel

To overcome the leaks of the macromodels presented earlier, a new macromodel was developed by Fabre and Alami [8]. The macromodel schematic is shown in Fig. 6. The model can be traced down to three stages, input stage, gain stage and output stage. This macromodel introduces new concepts over the two earlier ones

1. The frequency dependence of the output impedances of

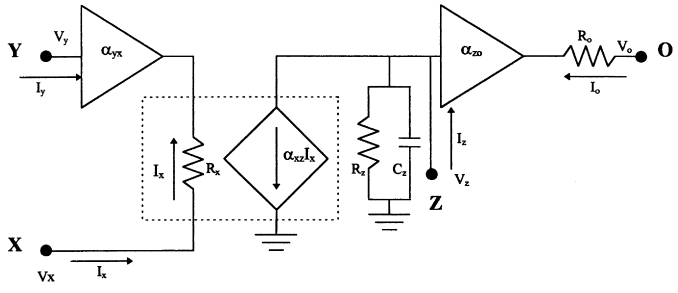

Fig. 4. A simple modeling of the non-idealities of the CFOA including the dominant parasitic effect.

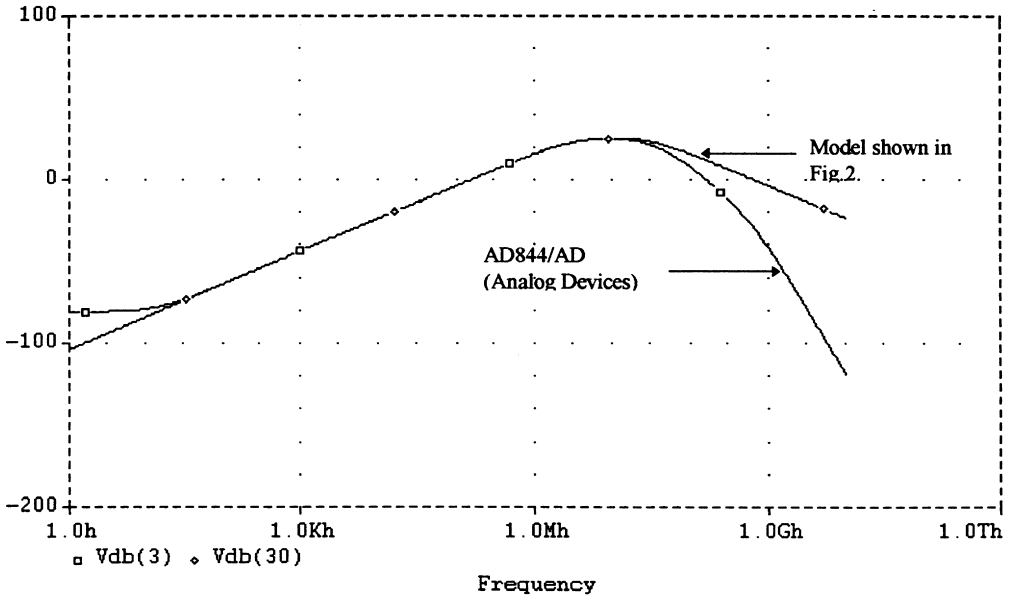

Fig. 5. The simulated response of the non-inverting differentiator shown in Fig. 2 for both the model shown in Fig. 4 and the AD844/AD.

the voltage followers modeled as a series combination of a resistor and an inductor.
2. The frequency limitation on the voltage and the current conveying properties modeled as finite simple poles that can replace the dominant poles found in actual CFOAs.
3. The parasitic grounded impedances seen at ports *Y* and *X*.
4. The change in the *Y* port impedance as a result of changing the operating point at the *X* terminal.

The mathematical equations that describe the model can be given as

$$I_y = V_y\left(\frac{1}{R_y} + sC_y\right) - \delta I_x \tag{3a}$$

$$V_x = \frac{\alpha_{yx}V_y + (R_x + sL_x)I_x}{1 + sC_xR_x + s^2C_xL_x} \tag{3b}$$

$$I_z = \frac{\alpha_{xz}I_x}{1 + sC_{xz}R_{xz} + s^2C_{xz}L_{xz}} + \left(\frac{1}{R_z} + sC_z\right)V_z \tag{3c}$$

$$V_o = \frac{\alpha_{zo}V_z}{1 + sR_{zo}C_{zo}} + (R_o + sL_o)I_o \tag{3d}$$

The parameters of the model can be measured as follows:

1. R_y and C_y will be determined with port *X* open, port *Z* grounded and port *Y* connected to a varying voltage source. By measuring the current flowing into port *Y*, R_y and C_y can be determined.
2. The value of δ can be calculated by connecting a grounded load across port *X* then measuring R_y again (to be denoted R_{YL}, and stands for R_y when there is a load connected to the *X* terminal). The value of δ can be thus given as

$$\delta = \left(R_y + R_x\right)\left(\frac{1}{R_{YL}} - \frac{1}{R_y}\right)$$

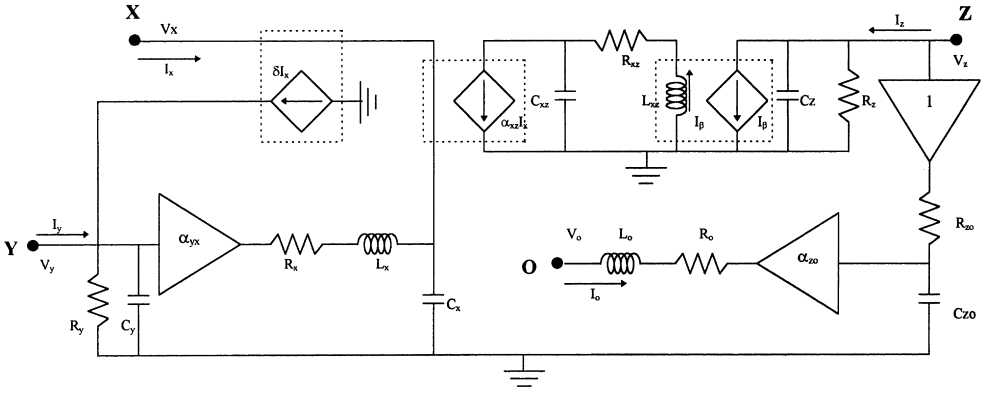

Fig. 6. The CFOA macromodel proposed in Ref. [8].

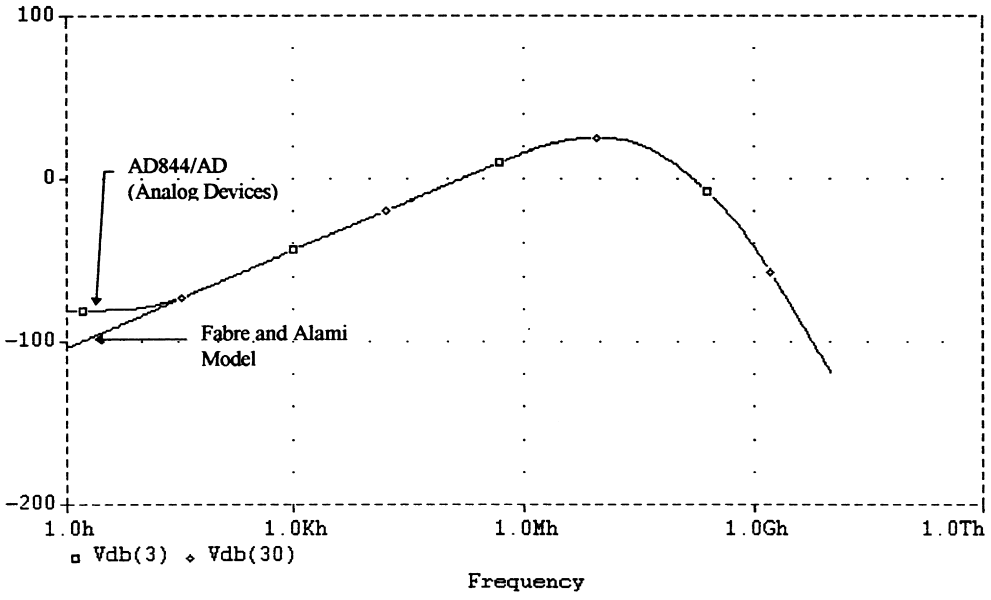

Fig. 7. The simulated response of the non-inverting differentiator shown in Fig. 2 for both the model presented in [1] and the AD844/AD.

where R_x is the output resistance at X measured at low frequency.

3. α_{yx} is the low-frequency voltage transfer ratio, it is measured with port X open and port Z grounded.
4. L_x and C_x will be calculated assuming a second order low-pass response with a peak (corresponding to a quality factor greater than 0.707) for the Y to X voltage transfer ratio. The resonant frequency and the quality factor of the response can be given by

$$\omega_o = \frac{1}{\sqrt{L_x C_x}} \quad \text{and} \quad Q = \frac{1}{R_x}\sqrt{\frac{L_x}{C_x}}$$

These are directly related to the measured characteristics of the peak magnitude of the response ($\beta_{\max}$ occurring at a frequency $\omega_{\max}$) through

$$\frac{\omega_{\max}}{\omega_o} = \sqrt{1 - \frac{1}{2Q^2}} \quad \text{and} \quad \frac{\beta_{\max}}{\beta_o} = Q\sqrt{1 - \frac{1}{4Q^2}},$$

where β_o is the magnitude at DC. If the quality factor was found to be less than 0. 707, the frequency response does not exhibit a peak. In this case, if deviations of the phase shift are acceptable, the response might be approximated to a first order transfer corresponding to $L_x = 0$ [8].

5. L_{xz} and C_{xz} can be calculated in a way similar to that used in the calculation of L_x and C_x (R_{xz} can be assumed 1 Ω).
6. R_z and C_z can be calculated in a way similar to that used in the calculation of R_y and C_y.
7. The product of $R_{zo}C_{zo}$ is the dominant pole of the transfer from Z to O and can be calculated by measuring the 3 dB bandwidth of the response.
8. The output impedance, R_o and L_o, can be measured by applying a varying voltage source to port Z and measuring the current flowing from port O being grounded.

The aforementioned parameters were measured for the AD844 from Analog Devices in [8] and the following

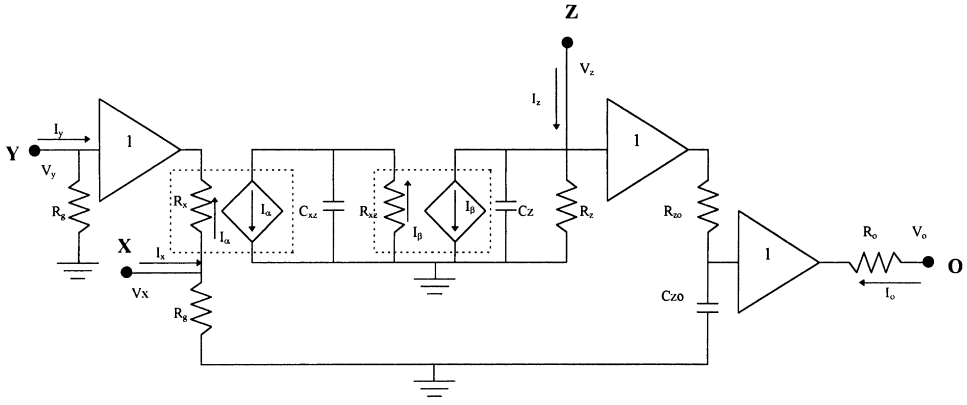

Fig. 8. The first proposed CFOA macromodel.

results were given:

$\alpha_{yx} = \alpha_{xz} = \alpha_{zo} \approx 1$

$R_y = 10\ \text{M}\Omega \quad C_y = 2\ \text{pF} \quad R_x = 50\ \Omega \quad L_x = 10\ \text{nH}$

$C_x = 2\ \text{pF}$

$R_{xz} = 1\ \Omega \qquad L_{xz} = 0 \qquad C_{xz} = 3.18\ \text{nF}$

$R_z = 3\ \text{M}\Omega \qquad C_z = 5.5\ \text{pF} \qquad R_{zo} = 1\ \Omega$

$C_{zo} = 0.318\ \text{nF}$

$R_o = 15\ \Omega \qquad L_o = 60\ \text{nH}.$

To test the accuracy of the model, simulation of the same non-inverting differentiator shown in Fig. 2 was carried out for both the aforementioned model and the model given by Analog devices in the PSpice library. The results are shown in Fig. 7. Clearly it represents the best results obtained so far although there is a deviation from the AD844 performance at low frequencies whose effect is to neglect a DC component present in the actual AD844 model.

5. The first proposed macromodel

This macromodel (Fig. 8) can be thought of as a modified workout of Fabre and Alami's macromodel that nearly maintains the good response equivalence at high frequency but overcomes the problem found in the former model at low frequency through a lower number of passive elements and controlled sources.

The main differences from the previous macromodel [8] can be summarized as:

1. The effect of the decrease of the Y impedance as a result of the X terminal load is neglected. The reason for such an approximation is that for typical CFOA the impedance seen at the input from the Y terminal is nearly infinite in the case of CMOS implementation and is very high (e.g. $R_y = 11\ \text{M}\Omega$ for the AD844 and 200 MΩ for the AD846) in case of bipolar implementations, also such an effect is present only in translinear input stages.
2. The finite frequency response between the Y port and the X port voltages was neglected. The reason for such an approximation is that for translinear input stages designed from high performance bipolar array the voltage following action between port Y and port X have a bandwidth that can go over gigahertz range [8].
3. A finite resistance is added from the X terminal to ground that simulates the effect of a voltage tracking error between terminals Y and X. In addition it fixes the deviation found at low frequencies with the former macromodel.
4. The effect of the increase in the output impedance of the voltage followers (from Y to X and from Z to O) is neglected and the output impedance is assumed purely resistive. This assumption is valid for a good degree of approximation for frequency ranges below a hundred megahertz (which is typical for a wide range of applications).

The mathematical equations that describe the model can be given as

$$I_y = \frac{V_y}{R_y} \tag{4a}$$

$$V_x = \left(V_y + R_x I_x\right)\left(\frac{R_g}{R_x + R_g}\right) \approx \left(1 - \frac{R_x}{R_g}\right)V_y + R_x I_x \tag{4b}$$

$$\begin{aligned} I_z &= \frac{I_x - \dfrac{V_x}{R_g}}{1 + sC_{xz}R_{xz}} + \left(\frac{1}{R_z} + sC_z\right)V_z \\ &\approx \frac{I_x}{1 + sC_{xz}R_{xz}} + \left(\frac{1}{R_z} + sC_z\right)V_z \end{aligned} \tag{4c}$$

$$V_o = \frac{V_z}{1 + sR_{zo}C_{zo}} + R_o I_o. \tag{4d}$$

The parameters of the model can be measured as follows:

1. R_y will be determined with port X open, port Z grounded and port Y connected to a voltage source. By measuring the current flowing into port Y, R_y can be determined. In the same process R_g can be measured by recording the ratio between voltages at terminals Y and X.
2. R_x can be measured by setting ports Y and Z to ground and applying a voltage source at terminal X. By measuring the current flowing into port X, R_x can be determined.
3. The product of $R_{xz}C_{xz}$ is the dominant pole of the transfer from X to Z and can be calculated by measuring the 3 dB bandwidth of the response (the same way used in calculating the X to Z transfer in [8]).
4. R_z and C_z can be calculated in a way similar to that used in the calculation of R_y (the same way used in calculating the R_z and C_z in [8]).
5. The product of $R_{zo}C_{zo}$ is the dominant pole of the transfer from Z to O and can be calculated by measuring the 3 dB bandwidth of the response.
6. The output impedance, R_o can be measured by applying a varying voltage source to port Z and measuring the current flowing from port O being grounded.

The aforementioned parameters were measured for the AD844 from Analog Devices and the results are given by

$R_y = 11\ \text{M}\Omega \qquad R_x = 50\ \Omega \qquad R_{xz} = 1\ \Omega$

$C_{xz} = 5.31\ \text{nF}$

$R_z = 3\ \text{M}\Omega \qquad C_z = 5.5\ \text{pF}$

$R_{zo} = 1\ \Omega \qquad C_{zo} = 0.318\ \text{nF} \qquad R_o = 15\ \Omega.$

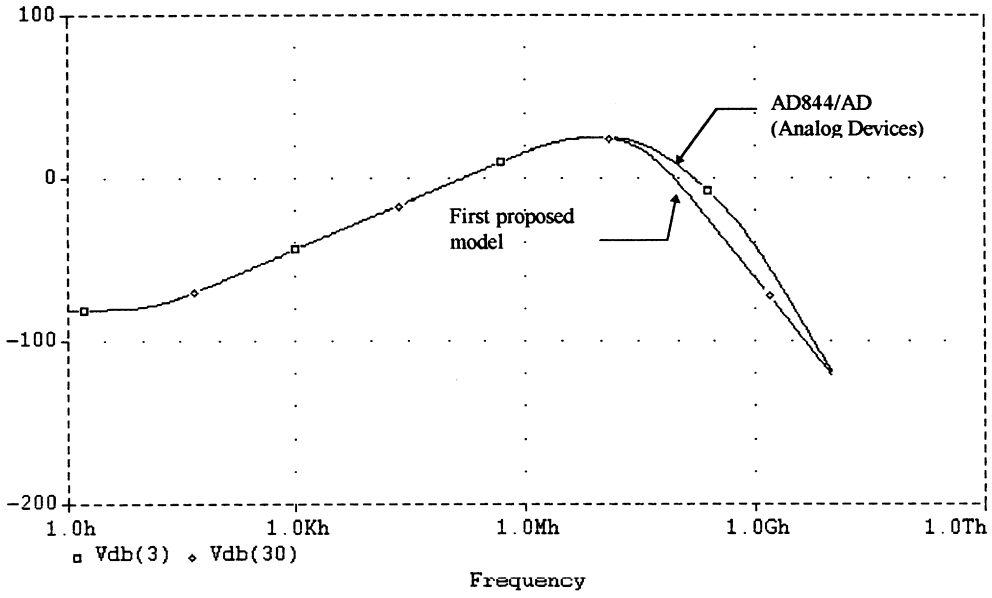

Fig. 9. The simulated response of the non-inverting differentiator shown in Fig. 2 for both the first proposed model and the AD844/AD.

To test the accuracy of the model, simulation of the same non-inverting differentiator shown in Fig. 2 was carried out for both the aforementioned model and the model given by Analog devices in the PSpice library. The results are shown in Fig. 9.

The results of the simulation performed shows that the presented model well agrees with the AD844 from DC up to 60–70 MHz. At high frequencies the macromodel developed in [8] is superior to that one on the expense of a much more complicated set of mathematical equations that describe the model (compare Eqs. (3a)–(3d) with Eqs. (4a)–(4d)).

The purpose of developing that model was to introduce a macromodel that is suitable for manual calculations yet quite accurate to a wide frequency range. To achieve simplicity of the mathematical calculations describing the model, it neglects several effects found in typical CFOAs (such as the frequency dependence of the output impedance of voltage followers). The approximations taken are typically of a second order nature and for typical CFOAs they are usually neglected for normal operating frequencies.

6. The second proposed macromodel

The second proposed macromodel (Fig. 10) uses a lower number of passive elements and controlled sources, yet achieves a performance superior to the last two models. The main difference between this model and the previous two is in the way of modeling the *X* to *Z* current conveying non-ideality. Practically there is no intrinsic finite pole for the current conveying between ports *X* and *Z*. Frequency

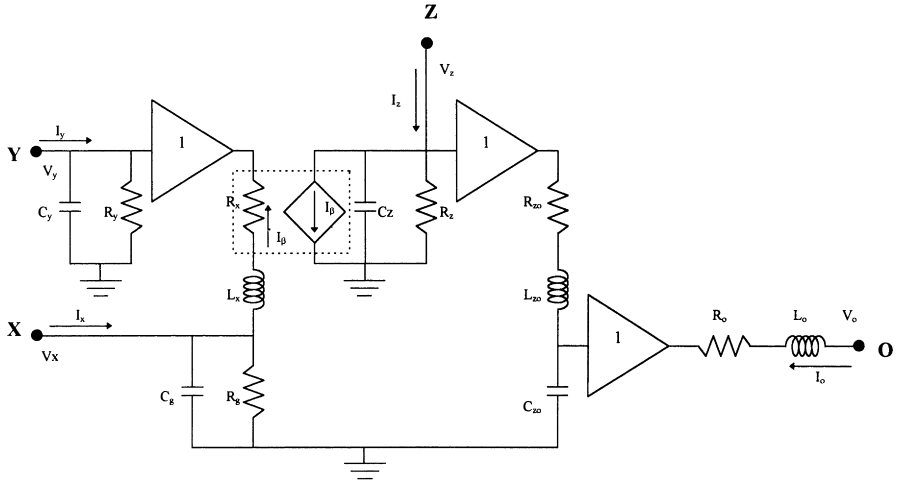

Fig. 10. The second proposed CFOA macromodel.

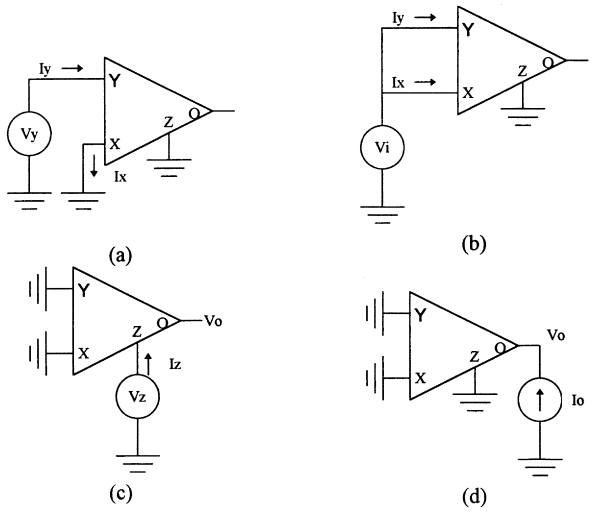

Fig. 11. The circuit configurations used in measuring the parameters of the second proposed macromodel: (a) Measuring R_y, C_y, R_x and L_x; (b) measuring R_g and C_x; (c) measuring R_z, C_z, R_{zo}, L_{zo} and C_{zo}; and (d) measuring R_o and L_o.

limitation is a result of the presence of parasitic effects (the effective parasitic capacitance seen between port X and ground C_x, the input resistance at the X terminal R_x). For this reason the finite pole between the X to Z current transfer ratio frequency response is not fixed, yet it changes with the loads present at terminals X and Z.

The second difference is in the introduction of a second order transfer between port Z and port O. Typically the voltage buffer between Z and O exhibits a second order or a higher transfer equation with a flat response having no peaks in magnitude (For the AD844 the Z to O voltage following property exhibits two simple poles one at 50 MHz and the other at 500 MHz.) Modeling the transfer with two poles gives a better performance over using one dominant pole.

The mathematical equations that describe the model can be given as

$$I_y = V_y\left(\frac{1}{R_y} + sC_y\right) \tag{5a}$$

$$V_x = \frac{V_y + (R_x + sL_x)I_x}{\left(1 + (R_x/R_g)\right) + s\left(C_gR_x + (L_x/R_g)\right) + s^2C_gL_x} \tag{5b}$$

$$I_z = I_x - \left(\frac{1}{R_g} + sC_g\right)V_x + \left(\frac{1}{R_z} + sC_z\right)V_z \tag{5c}$$

$$V_o = \frac{V_z}{1 + sR_{zo}C_{zo} + s^2L_{zo}C_{zo}} + (R_o + sL_o)I_o. \tag{5d}$$

Parameter measuring is accomplished through the circuit configurations shown in Fig. 11. The parameters of the model can be measured as follows:

1. R_y, C_y, R_x and L_x can be measured using the configuration shown in Fig. 11(a) as follows:

$$\frac{I_y}{V_y} = \frac{1}{R_y} + sC_y \qquad \frac{V_y}{I_x} = R_x + sL_x.$$

2. R_g and C_x can be measured using the configuration shown in Fig. 11(b) as follows:

$$\frac{I_x}{V_i} = \frac{1}{R_g} + sC_g.$$

3. R_z and C_z can be measured using the configuration shown

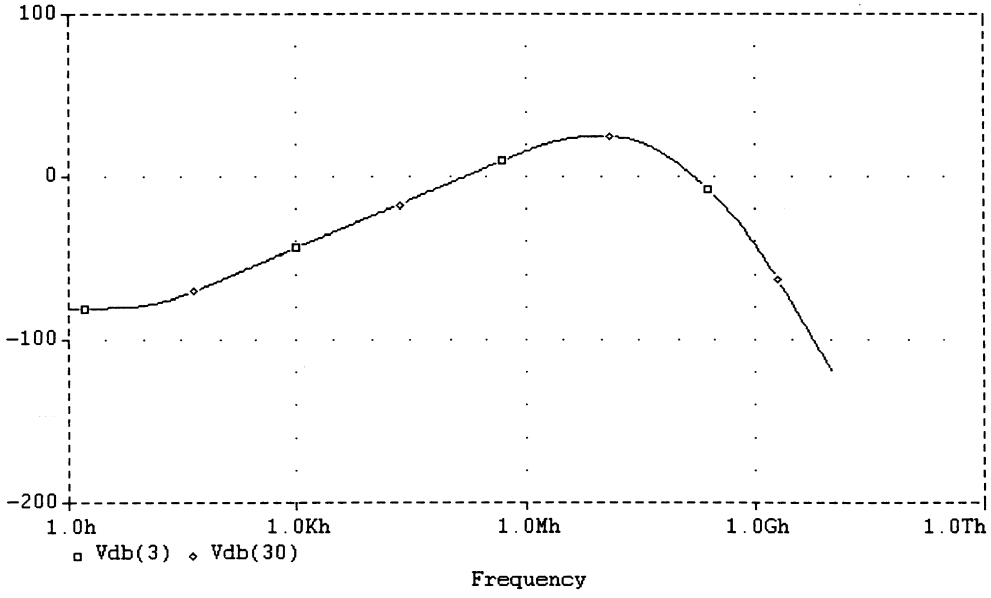

Fig. 12. The simulated response of the non-inverting differentiator shown in Fig. 2 for both the second proposed model and the AD844/AD.

in Fig. 11(c) as follows:

$$\frac{I_z}{V_z} = \frac{1}{R_z} + sC_z.$$

As for the output stage, the first two dominant poles found in the response between V_z and V_o can be modeled by choosing the element values as follows:

$$\frac{L_{zo}}{R_{zo}} = \frac{1}{\omega_1 + \omega_2} \qquad R_{zo}C_{zo} = \frac{1}{\omega_1} + \frac{1}{\omega_2}.$$

(R_{zo} can be arbitrarily chosen as 1 Ω.) Note that if the second pole is very far compared to the first pole L_{zo} can be neglected and the output stage reduces to a simple RC first-order section.

4. R_o and L_o can be measured using the configuration shown in Fig. 11(d) as follows:

$$\frac{V_o}{I_o} = R_o + sL_o.$$

The aforementioned parameters were measured for the AD844 from Analog Devices and the results are given by

$R_y = 11\ \text{M}\Omega \qquad C_y = 0$

$R_x = 50\ \Omega \qquad L_x = 10\ \text{nH} \quad C_g = 2\ \text{pF} \qquad R_g = 11\ \text{M}\Omega$

$R_z = 3\ \text{M}\Omega \qquad C_z = 5.5\ \text{pF}$

$R_{zo} = 1\ \Omega \qquad C_{zo} = 3.5\ \text{nF} \qquad L_{zo} = 0.29\ \text{nH}$

$R_o = 15\ \Omega \qquad L_o = 60\ \text{nH}.$

To test the accuracy of the model, simulation of the same non-inverting differentiator shown in Fig. 2 was carried out for both the aforementioned model and the model given by Analog devices in the PSpice library. The results are shown in Fig. 12.

The results of the simulation performed indicate that the presented model gives the highest degree of accuracy compared to the previous models, yet it is not as simple as the first proposed macromodel when dealing with manual calculations.

All macromodels presented for the AD844-CFOA in this section requires much lower simulation time than the one supplied by Analog Devices.

7. Conclusions

Two new SPICE macromodels for the CFOA were presented. The models accurately describe the behavior of a typical CFOA over a wide frequency range. The first proposed macromodel is more suitable for manual calculations due to its fairly simple mathematical representation model. The second proposed macromodel is more suitable for SPICE simulation as its mathematical description is more complex than that of the first presented model. It is more accurate than the first proposed model at high frequencies. Both presented macromodels describe the CFOA at low frequencies better than previously presented macromodels and they use a lower number of passive elements and controlled sources, hence exhibits a lower simulation time than the model presented in [8]. Simulation carried out over a non-inverting differentiator test circuit using the AD844-CFOA from Analog Devices as an example showed that the behavior of both macromodels are accurate for a wide range of frequencies as compared to the model supplied from Analog Devices.

References

[1] A.M. Soliman, Applications of the current feedback operational amplifier, Analog Integrated Circuits and Signal Processing 11 (1996) 265–302.
[2] C. Chang, C.S. Hwang, S.H. Tu, Voltage-mode notch, lowpass and bandpass filter using current-feedback amplifiers, Electron. Lett. 30 (24) (1994) 2022–2023.
[3] I. Liu, High input impedance filters with low component spread using current-feedback amplifiers, Electron. Lett. 31 (13) (1995) 1042–1043.
[4] S.I. Liu, Universal filter using two current-feedback amplifiers, Electron. Lett. 31 (8) (1995) 629–630.
[5] H. Palouda, Current feedback amplifiers, National Semiconductor application notes 597, 1989.
[6] Analog Devices, Linear Products Data Book, Norwood, MA, 1990.
[7] C. Toumazou, J. Lidgey, A. Payne, Emerging techniques for high frequency BJT amplifier design, a current-mode perspective, First International Conference on Electronics, Circuits and Systems, Cairo, Egypt, 1994.
[8] A. Fabre, M. Alami, A precise macromodel for second generation current conveyors, IEEE Trans. Circuits Syst. I 44 (7) (1997) 639–642.
[9] S. Jost, V. Hibner, Spice current feedback amplifier macro-model, Harris Semiconductor application notes HA5004, 1991.
[10] R. Mancini, J. Lies, Current feedback amplifier theory and applications, Harris Semiconductor application notes, No. AN9420, 1995.
[11] R. Mancini, Comparison of current feedback opamp SPICE models, Harris Semiconductor application notes HA5013, 1996.
[12] National Semiconductor, Development of an extensive SPICE macromodel for current feedback amplifiers, National Semiconductor application notes 840, 1992.
[13] R. Schmid, Stability analysis of current-feedback opamp, National Semiconductor application notes OA-25, 1995.